Mathematical Biosciences and Engineering

http://www.aimspress.com/journal/MBE

MBE, 16(6): 7057–7084.
DOI: 10.3934/mbe.2019354
Received: 05 June 2019
Accepted: 25 July 2019
Published: 01 August 2019

Research article

On the mechanism of antibiotic resistance and fecal microbiota transplantation

Xiaxia Kang[1], Jie Yan[2], Fan Huang[3] and Ling Yang[1,2,*]

[1] School of Mathematical Sciences, Soochow University, Suzhou 215006, P. R. China
[2] Center for Systems Biology, Soochow University, Suzhou 215006, P. R. China
[3] Mathematics Application Joint Laboratory of Soochow University and Suzhou Jiaoshi Intelligence Technology Co., Ltd, Soochow University, Suzhou 215006, P. R. China

* **Correspondence:** Email: lyang@suda.edu.cn; Tel: +8613913152842.

Abstract: Antibiotic resistance is a growing threat to human health and is caused by mainly the overuse of antibiotics in clinical medicine. Clinically, drug resistance emerges after a series of antibiotic treatments, implying that each treatment changes the intestinal flora composition and the accumulations of these changes induce the resistance. But mathematically, this cumulative effect cannot be achieved by a general population model, because the system will return to its pre-treatment state (an isolated steady state) after each cure. Based on the fact that sensitive bacteria and resistant bacteria are similar in most respects except their reactions to antibiotics, we developed a mathematical model with a specific phase-space structure: instead of isolated points, the steady states of this system compose one-dimensional manifolds (line segments). This structure explains the fundamental mechanism of antibiotic resistance: after antibiotic treatment, the system cannot return to the pretreatment healthy steady state but rather slightly moves along the manifold to a different steady state. Each use of antibiotics can change the ratio of resistant to susceptible pathogens in the host. The change the ratio can persist and accumulate, and finally promotes the emergence of antimicrobial resistance. We also assessed key factors (such as pathogen composition, the amount and composition of beneficial bacteria, medication duration and bactericidal rates of drugs) influencing the development of drug resistance. In addition, we clarified how fecal microbiota transplantation affects the treatment of antibiotic-resistant infections. The effect is essentially a transfer towards the healthy state in the phase space. Finally, based on the mechanisms revealed by the mathematical models, we suggested some strategies to delay or prevent the emergence of drug resistance. These findings not only provide a solid theoretical basis for the treatment of antimicrobial resistance, but also inspire clues to the phenomenon of drug resistance.

Keywords: drug resistance; fecal microbiota transplant; pathogens; bistability; dynamic model

1. Introduction

Drug-resistant infection caused by over use of antibiotic is one of the most serious health problems of the 21st century. In the United Sates in 2005, a data survey showed that the total number of deaths caused by methicillin-resistant *Staphylococcus.aureus* invasion exceeded that caused by HIV/AIDS in the same year. A recent estimate suggested that at least 700,000 patients worldwide die from antibiotic resistance every year. These alarming situations highlight the need to explore the formation mechanism of antibiotic resistance to control the incidence of resistance.

As a standard treatment for various diseases, antibiotics have been widely used in the clinic due to their convenience and quick action. Standard antibiotic treatment guidelines aim to maximize treatment efficacy and minimize side effects, but they do not give enough consideration to the long-term impact, such as the emergence of antibiotic resistance. In fact, an increasing-number of studies have demonstrated that antibiotic use can alter the composition of the gut microbiota [1–3]. Some studies have shown that the microbiota composition in patients treated with antibiotics cannot return to the pretreatment state [4–6]. Additionally, a growing body of literature has suggested that antibiotic-resistant pathogens are enriched in the intestinal microbiota of patients with high antibiotic usage [7]. More generally, it has been demonstrated that altering the composition of the microbiota will interfere with some of the human-microbe interactions that are integral to human physiology. However, the fundamental role of the microflora composition has not been fully explored in the development of antibiotic resistance.

The harmony of the gut microbiota ecosystem is crucial to host health. As the dominant microorganisms in the whole intestinal flora, probiotics are very important in maintaining the balance of the gut microbiota. Several studies of intestinal flora have demonstrated that beneficial bacteria play an essential role in intestinal health. For example, beneficial bacteria can inhibit the reproduction and growth of pathogens or prevent the invasion of foreign pathogens by secreting bacteriocins or activating the host's immune defense system [8–10]. Altogether, exploring the mechanism of antibiotic resistance must take into account the role of probiotics.

FMT (short for Fecal microbiota transplantation) as a new therapy is one of the main treatments against drug-resistant infections. FMT is a therapeutic regimen of infusion of fecal preparation from a healthy donor into a patient to cure a certain disease [11]. The gut microbiota in healthy donors is dominated by a large number of probiotics. Therefore, FMT is a feasible strategy to resist drug resistance. Recently, FMT has gradually been adopted and has achieved considerable success in curing antibiotic-resistant infections [12–16]. For instance, many studies have shown that FMT restored both the gut microbiota composition and function in patients who suffered from recurrent *Clostridium difficile*-associated diarrhea [17–19]. Some studies have shown that the worldwide mean cure rates of FMT for diarrhea are approximately 91% [20]. Increasing use as a first-line treatment suggests that FMT combined with antibiotic treatment can be effective in treating infections caused by "superbugs" [12, 13]. Therefore, understanding the effective mechanism of FMT is another important issue.

Mathematical modeling is a powerful tool to interpret the development of antibiotic resistance. Some studies have used dynamic systems approaches to explore the growth patterns of microbial species, species-species interactions, and susceptibilities of the intestinal microbiota to antibiotics [21–23]. Other researchers have proposed multi-stability or the existence of strongly

interacting species to explain the microbial compositional shift caused by antibiotic treatments [24, 25]. However, most quantitative studies of the intestinal microbiota are limited to the classification of microorganisms into antibiotic-sensitive and antibiotic-resistant bacterial groups, and the critical effects of probiotics are absent [26–29]. Additionally, the theoretical analysis of fecal bacteria transplantation is sparse.

Unlike previous studies, we focused on the case where gene sequences of sensitive and resistant pathogens differ at only one site or a few sites in the drug resistance determinant region. This situation has been confirmed by deep sequencing technology in many cases. For example, the difference between methicillin-resistant *Staphylococcus aureus* and non-resistant strains is that a site mutation occurs in the -10 consensus of the promoter [30]. Another example is that there was no significant difference in growth between NDM-1-expressing *E.coli* (which are resistant to all β-lactam antibiotics except monobactams) and their isogenic parental strains [31]. We also considered the role of probiotics in maintaining the balance of the gut microbiota. Therefore, we modeled the combined effects of inter-specifies interaction (probiotics and pathogens) and antibiotic therapy (or FMT combined with antibiotic treatment) to explore the mechanism of development of drug resistance and the mechanism of FMT. In our model, the intestinal microbiota was divided into the following three groups: probiotics, sensitive-pathogens and resistant-pathogens. Specifically, we wanted to explore the dynamic evolution of the core gut microbiota, to provide critical information for the optimal use of antibiotics to delay or even prevent the emergence of antibiotic resistance. By mathematical modeling and numerical simulations, we demonstrated the importance of probiotics and interspecies inhibition in the development of antibiotic resistance. This work clarified that the mechanism of FMT is essentially a transfer towards the healthy states in the phase space. In addition, we also suggested some strategies (i.e., early usage of FMT) to delay or prevent the emergence of drug resistance. These findings provide novel insights for understanding drug resistance and FMT.

2. Dynamic model

We used the generalized Lotka-Volterra (L-V) equation to establish a time-dependent ecological dynamic model with external disturbances (antibiotics). The human intestinal microbiota is a complex and dynamic ecosystem of crucial importance to human health. In this study, we were primarily interested in the development of antibiotic-resistance which is caused by changes in the microbiota composition state. To achieve this goal, we classified the microbiota into three groups (probiotics, antibiotic-sensitive pathogens and antibiotic-resistant pathogens) to represent the response of commensal bacteria to antibiotic treatments.

Experimental studies have shown that microbial growth and reproduction will eventually saturate due to limited resources and space [32, 33]. Therefore, we introduced a logistic equation to depict the growth pattern of bacteria under limitation of resources. Some studies on microbial interactions have shown that probiotics can effectively inhibit the growth of pathogens and the formation of pathogenic spores by secreting bacteriocins or short-chain fatty acids and so on; in turn, pathogens can also secrete toxins to eliminate probiotics [9, 34–36]. Combining these existing experimental phenomena, we developed a model in which pathogens (consisting of antibiotic-sensitive pathogens and antibiotic-resistant pathogens) and probiotics (i.e., B_1) inhibited each other, as shown in Figure 1. Our system further considered the competition for resources between sensitive pathogens and resistant

pathogens with population sizes of P_{S1} and P_{T1}, respectively. The ecological dynamic model assumes that three populations follow a set of ordinary differential equations:

$$\begin{cases} \frac{dP_{S1}}{dt} = r_1(1 - \frac{k_1P_{S1}+k_2P_{T1}}{K_1})P_{S1} - k_{12}\frac{B_1^2}{B_1^2+a'^2}P_{S1} - d_1P_{S1} - \eta_1P_{S1} \\ \frac{dP_{T1}}{dt} = r_1(1 - \frac{k_1P_{S1}+k_2P_{T1}}{K_1})P_{T1} - k_{12}\frac{B_1^2}{B_1^2+a'^2}P_{T1} - d_1P_{T1} - \eta_2P_{T1} \\ \frac{dB_1}{dt} = r_2(1 - \frac{B_1}{K_2})B_1 - k_{21}\frac{(k_1P_{S1}+k_2P_{T1})^2}{(k_1P_{S1}+k_2P_{T1})^2+b'^2}B_1 - d_2B_1 - \eta_3B_1 \end{cases} \tag{2.1}$$

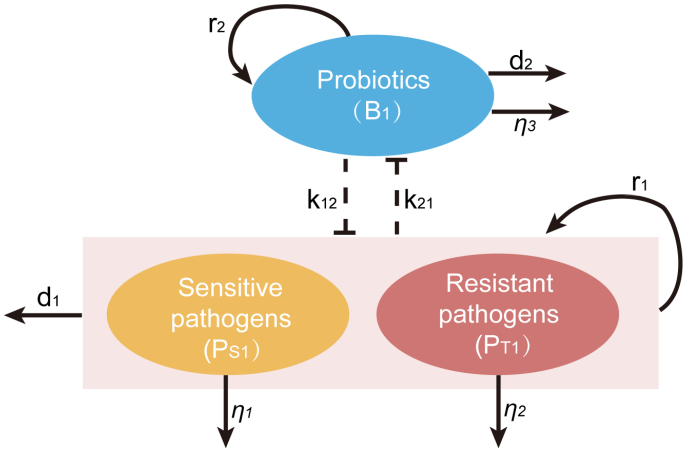

Figure 1. The three-group model of the intestinal microbiota with sensitive pathogens, resistant pathogens and probiotics. The blue oval is the population of probiotics. The pink rectangle is the population of pathogens that consists of two groups of pathogens: sensitive pathogens and resistant pathogens. Both pathogens compete for the same growth substrates, which are different from those for the probiotics. The outflow arrows denote the possible fates of different strains. The model parameters r_1 and r_2 represent growth rates. The death rates d_1 and d_2 consist of the immune response killing bacteria and fecal efflux. η_j $(j = 1, 2, 3)$ describes killing rate of antibiotic. The dashed lines represent the inter-specifies inhibition between pathogens and probiotics (i.e., parameters k_{12} and k_{21}).

A key assumption of our model is that sensitive pathogens and resistant pathogens have differences in one site or very few sites in the gene coding sequence, which mainly affect the bactericidal activity of antibiotics. Actually, using deep sequencing technology, this situation has been confirmed in many cases [30, 31]. For instance, the resistant strains have only one site mututaion from the non-resistant *Staphylococcus aureus*. The genetic determinant of resistance, mecA, is a gene of *methicillin − resistant Staphylococcus aureus*. DNA sequence of mecA from homologous resistant strains revealed that this resistance originated from a site mutation in the -10 consensus of the promoter, that is, thymine residues of sensitive strains (i.e., T at nt 1577) were replaced by adenine of resistant strains (i.e., A at nt 1577) [30]. Additionally, Stephan Gottig, et al. used a vivo infection

model to study the growth kinetics of NDM-1-expressing *E.coli* and their isogenic controls [31]. The results showed that there was no significant difference in growth. Therefore, we assume that the relevant parameters of these two pathogens (sensitive and resistant) are identical except for antibiotic bactericidal rates (η_1 and η_2) and competition coefficients (k_1 and k_2). In our model, this assumption is the basis of explaining the mechanism of drug resistance.

Here, r_i and d_i are the growth rate and the mortality rate of pathogens and probiotics ($i = 1, 2$), respectively. We introduce a logistic function to characterize the growth of probiotics and two types of pathogens. The term in brackets indicates that the growth of every species is limited by the maximum population size K_1 (K_2). k_1 and k_2 denote the inter-specific competition intensity of the two pathogen groups because they will compete for the same nutritional resources and space. The interspecific inhibitions between probiotics and pathogens, mediated through secretion (bacteriocin or toxins), are represented by increasing Hill functions. The inhibition coefficients k_{12} (pathogens by probiotics) and k_{21} (probiotics by pathogens) indicate the maximum inhibition intensity of bacteriocin and toxins, respectively. The parameter $a^{'}$ (or $b^{'}$) is probiotic (or pathogen) population that gives half of the maximum inhibition coefficient k_{12} (or k_{21}). The last item in the equations describes the mortality rate caused by antibiotic intake. Many studies have shown that resistant pathogens can prevent the entry of antibiotics different ways, as follows: altering cell membrane permeability, changing protein structure in the body to inhibit binding, or secreting certain hydrolytic enzymes to break down antibiotics [37–39]. Therefore, we assumed that antibiotics have different effects in different species, i.e., the drug bactericidal rate η_j of species j (=1, 2 or 3) is different for different species (or η_j is the antibiotic-related death rate).

It is convenient to scale the variables and set the maximum capacity to unity ($K_1 = K_2 = 1$). By introducing $P_S = P_{S1}/K_1$; $P_T = P_{T1}/K_1$; $B = B_1/K_2$; $a = \frac{a^{'}}{K_2}$; and $b = \frac{b^{'}}{K_1}$, we simplified the Eq (2.1) to obtain the following model:

$$\begin{cases} \dfrac{\mathrm{d}P_S}{\mathrm{d}t} = r_1[1-(k_1P_S+k_2P_T)]P_S - k_{12}\frac{B^2}{B^2+a^2}P_S - d_1P_S - \eta_1P_S \\ \dfrac{\mathrm{d}P_T}{\mathrm{d}t} = r_1[1-(k_1P_S+k_2P_T)]P_T - k_{12}\frac{B^2}{B^2+a^2}P_T - d_1P_S - \eta_2P_T \\ \dfrac{\mathrm{d}B}{\mathrm{d}t} = r_2(1-B)B - k_{21}\frac{(k_1P_S+k_2P_T)^2}{(k_1P_S+k_2P_T)^2+b^2}B - d_2B - \eta_3B \end{cases} \tag{2.2}$$

Different growth rates or mortality rates are used to characterize the different physiological stages. In the healthy stage, we set the drug bactericidal rate η_j as zeros in Eq (2.2), because there is no antibiotic involved. In the infection stage, increased r_1 was used to describe the accumulation of the pathogens. For the antibiotic treatment stage, we utilized nonzero drug bactericidal rates, η_j ($j = 1, 2$ or 3), to present the effects of antibiotics. For the FMT treatment stage, we introduced the survival rate coefficient k ($0 < k < 1$) to characterize the effect of fecal microbiota transplantation. For example, the microbiota composition state before FMT and that of donors are (P_S, P_T, B) and (P_{Sh}, P_{Th}, B_h), respectively, and the instantaneous composition state after FMT becomes $(P_S + k * P_{Sh}, P_T + k * P_{Th}, B + k * B_h)$. In the recovery stage, the same parameters as in the healthy stage were used. Table 1 summarizes the values of all the parameters used in the Eq (2.2) and the corresponding parameter values for different stages.

Table 1. List of Parameters and their values.

Symbols	Definition	Value (day^{-1})
r_1	Growth rate of pathogens	0.664 (without infection)
		$0.664 * 1.32$ (with infection)
r_2	Growth rate of probiotics	0.718
d_1	Death rate of pathogens	0.0501
d_2	Death rate of probiotics	0 .0751
k_{12}	Maximum inhibition coefficient of probiotics on pathogens	0.76
k_{21}	Maximum inhibition coefficient of pathogens on probiotics	0.84
k_1	Competitive coefficient of P_T against P_S	0.5
k_2	Competitive coefficient of P_S against P_T	0.5
a	Probiotics amount that yields 50% of k_{12}	0.58
b	Pathogens amount that yields 50% of k_{21}	0.58
η_1	Killing rate of antibiotic for P_S	0.086 (with antibiotic)
η_2	Killing rate of antibiotic for P_T	0.0016 (with antibiotic)
η_3	Killing rate of antibiotic for probiotics	0.015 (with antibiotic)
k	Survival rate of fecal microbiota	0.5

3. Results

3.1. Validation of antibiotic resistance and effectiveness of FMT

We first characterized the host's complete physiological process of illness (red curve ①), drug treatment (sky blue curve ②), FMT (green curve ③) and recovery (blue curve ④) through time evolution curves of the total amount of pathogens (sensitive pathogens and resistant pathogens) (Figure 2A). Some studies have shown that each healthy individual harbors a stable gut microbiota [40]. Therefore, in our model, before the illness stage, the microbiota composition state was set in a healthy stable state, i.e., the amount of pathogens remained in a low level (-7 days to 0 days in Figure 2A). To depict the illness process, we used the overgrowth of pathogens, i.e., parameter r_1 became $1.32 * r_1$. In the illness stage, the pathogen populations continued to increase. Then, antibiotic treatment started on the fourth day after the infection and lasted for 3 days. We defined a course of continuous-medication for 3 days as a standard treatment, because many clinical trials have confirmed that most common infectious diseases can be cured with 3 days of drug therapy. Here, we assumed that the antibiotic effects (non-zero η_j) were added to the system to eliminate pathogens in this stage. In the meantime, the reproductive rate of pathogens was also effectively suppressed and returned to the healthy level (r_1). After drug treatment, the total amount of pathogens was significantly reduced to a lower level than that prior to treatment. From the 7^{th} day, the system entered the self-repair stage and then fully recovered after a long time. In the recovery process, we set the drug bactericidal rate (η_j) to zero because the bactericidal activity of antibiotic also disappears after drug withdrawal.

Figure 2A shows the first sixteen complete illness-treatment processes of the same patient. It can be seen intuitively that the amount of pathogens after the first 15 antibiotic treatments can return to the

pretreatment state. However, the amount of pathogens after the 16^{th} treatment can stabilize to a higher level (Figure 2A).

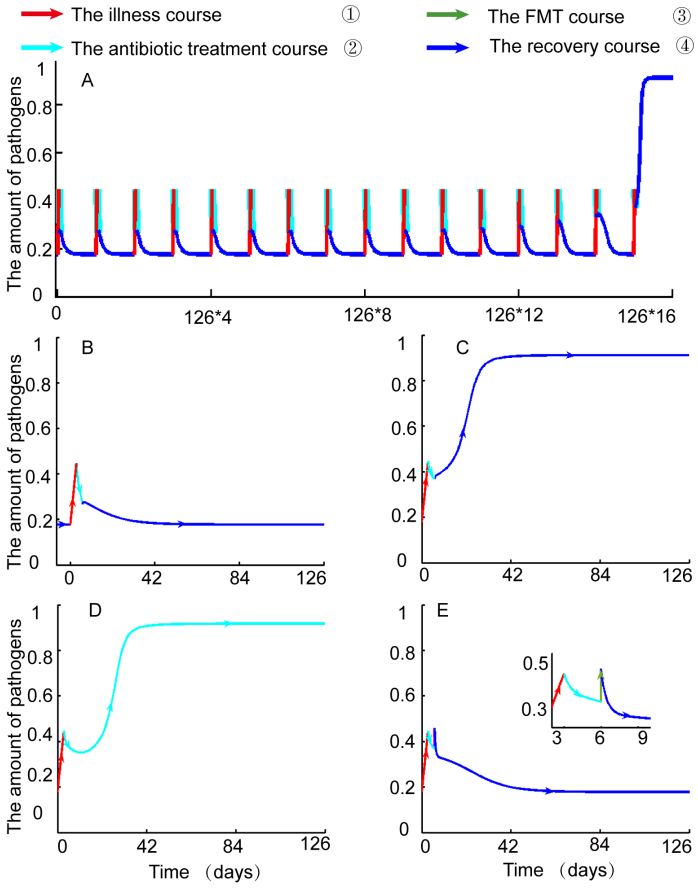

Figure 2. Time evolution curves of the total amount of pathogens in the illness-treatment processes. (A) The first 16 illness-treatment processes. (B) The first illness-treatment process. (C) The 16^{th} illness was not prevented by a 3-day medication course. (D) The 16^{th} infection was not prevented by a 4-month medication course. (E) The 16^{th} infection was treated with FMT combined with antibiotic. The arrow lines represent the illness course (red), the drug treatment course (sky blue), the FMT course (green) and the recovery or health course (blue). This figure shows that our model is reasonable and effective.

To further explore why the same treatment can work for only the first 15 times on the same disease, we amplified the details of the first and 16^{th} treatments (Figure 2B and C). After the first antibiotic treatment, the amount of pathogens rapidly decreased to a low level and reached a healthy stable state soon afterwards (Figure 2B). The patient accepted the same treatment after the 16^{th} infection, and the amount of pathogens eventually returned to a high level (the illness stable state) (Figure 2C). The 16^{th} treatment failure implies that the gut microbiota may have developed resistance or pseudo-resistance.

We then confirmed that the antibiotic lose efficacy in the 16^{th} infection is due to the emergence of drug-resistance. Upon the 16^{th} infection, we prolonged the duration of antibiotics treatment from 3 days to 4 months (the sky blue curve in Figure 2 D), however, the amount of pathogens still remains at

a high level (the illness stable state). The result shows that the amount of pathogens still rebounds to the illness state (the high stable state) even when the permanent treatment was given. Combining the data from the standard treatment and permanent treatment after the 16^{th} illness, these results suggest that the gut microbiota has already developed permanent resistance.

We further studied the improved strategy of FMT (i.e., FMT with antibiotic treatment). The results demonstrate that the amount of pathogens returned to the healthy level in our model (Figure 2E). Therefore, this simulation also reproduced that drug-resistant infections can be eliminated by FMT in clinic. In the amplified details, the total pathogens decreased slightly after antibiotic intake, but instantly rose to higher levels after the inoculation of fecal bacteria and subsequently rapidly declined. These simulation results are consistent with experimental observations in mouse models by Chaysavanh and Jens et al [41].

Therefore, these simulation results confirmed that our model can be used to explore the mechanism of antibiotic-resistance and the effectiveness of FMT. By revealing the dynamic evolution of the gut microbiota, we could provide new ideas for how to reduce the risk of drug resistance in clinical treatments.

3.2. The development mechanism of drug resistance

We first analyzed steady states to understand key features of this dynamic system, because the measurements of the gut microbiota composition in some studies typically represent steady state behaviors. Many experimental observations have indicated that the microbial ecosystem of each individual has a relatively stable and resilient community [4, 5, 42, 43]. Unless a large perturbation (e.g., antibiotic intake) is introduced, the ecological system remains stable for months or even years. The steady state of ecological dynamics system Eq (2.2) are those positive real solutions that satisfy equations set Eq (2.2). Because sensitive and resistant pathogens in the ecological system Eq (2.2) share the same parameters in the absence of antibiotic intake, we can combine these two variables together to form a new variable $P = k_1 * P_S + k_2 * P_T$. Therefore, we recast system Eq (2.2) to an equivalent two-dimensional system Eq (3.1),

$$\begin{cases} \dfrac{\mathrm{d}P}{\mathrm{d}t} = r_1(1-P)P - k_{12}\dfrac{B^2}{B^2+a^2}P - d_1P \\ \dfrac{\mathrm{d}B}{\mathrm{d}t} = r_2(1-B)B - k_{21}\dfrac{P^2}{P^2+b^2}B - d_2B \end{cases} \tag{3.1}$$

in which P indicates the weighted total population of two pathogens.

Then, we focused on this equivalent 2-D system Eq (3.1) to study the steady states. Under some constraint conditions, the system has six steady states, named P_0, P_{01}, P_{30}, P_1, P_2 and P_3. Under the parameter values of Table 1, we can get two eigenvalues of the system at each equilibrium point approximately. By caculating the Jacobian matrix of Eq (3.1) at these steady states, we obtained their eigenvalues. The numerical results showed that steady states P_1 and P_3 are locally asymptotically stable (because eigenvalues at both equilibrium points are negative real roots), and the rest are unstable (Figure 3A). And the two eigenvalues at the equilibrium point P_2 are one positive real root and one negative real root, respectively. Therefore, P_2 is a saddle point. Here, we are particularly interested in three biologically meaningful steady states: a healthy stable state (P_1) with probiotics dominant, a disease stable state (P_3) with pathogens dominant and an unstable state (P_2).

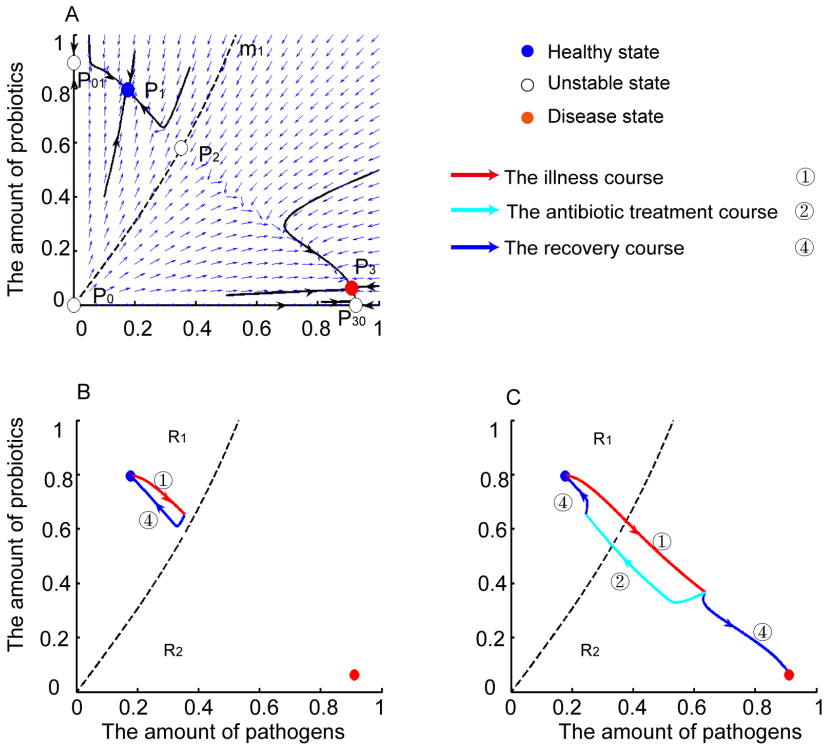

Figure 3. The vector field diagram in the P-B plane and disease types. (A) Phase plane analysis of the bistability, for the following parameters values: $r_1 = 0.664$; $r_2 = 0.718$; $d_1 = 0.0501$; $d_2 = 0.0751$; $k_{12} = 0.76$; $k_{21} = 0.84$; $a = 0.58$; and $b = 0.58$. Over the blue arrows describing the flow field in the phase-portrait (P-B), the black dashed curve is a stable manifold of a saddle (P_2). The equilibrium P_1 (blue circle, the healthy state) and equilibrium P_3 (red circle, the disease state) are stable nodes, and the remaining equilibriums (P_0, P_{01}, P_{30} and P_2) are unstable. In addition, the stable manifold is also a critical line between regions R_1 and R_2. (B) Self healing disease. The trajectory in the infection course remains in the area R_1. (C) Non-self-healing disease. The trajectory in the infection course passes through the manifold m_1 and enters into the area R_2.

A one-dimensional stable manifold (m_1) of the saddle point (P_2) can divide the first quadrant of the phase plane into two regions (R_1 and R_2). The vector field in Figure 3 depicts the long-term behavior depending on the initial conditions. The trajectories from the initial points in R_1 will converge towards the healthy stable state (P_1), but the trajectories from R_2 will ultimately reach the disease stable state (P_3). Therefore, we call the region R_1 as the self-healing area, and the region R_2 as the non-self-healing area.

In fact, this stable manifold (m_1) is also the boundary between the self-healing area and the non-self-healing area. After infection, the trajectory moved away from healthy stable state in our model. If the trajectory crossed this manifold m_1 during the illness, it approached the disease stable state (P_3) without treatment (the long blue curve in Figure 3C). In our model, we defined this disease as the non-self-healing disease in Figure 3C. In contrast, if the trajectory did not cross this manifold m_1 during

the illness, it returned to the healthy stable state even without treatment (blue curve in Figure 3B). The second case is the self-healing disease. Once the host infected with the non-self-healing disease, he had to be treated. The force of antibiotic treatment in our model pushes the trajectory back to above the critical manifold (e.g., the sky blue curve in Figure 3C).

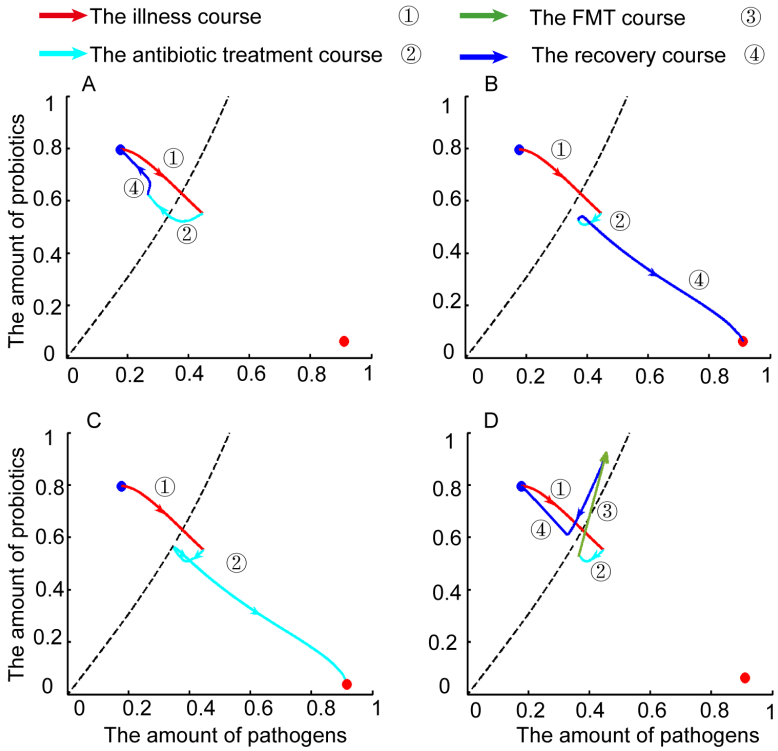

Figure 4. The illness-treatment-recovery processes in the phase plane. (A) The first infection was eliminated by a 3-day medication course. (B) The 16^{th} infection was not prevented by a 3-day medication course. (C) The 16^{th} infection was also not prevented by a 4-month medication course. (D) The 16^{th} infection was eliminated by FMT combined with antibiotic. The characteristic of antibiotic resistance is that the trajectory of the drug treatment course never crosses the manifold (the black dashed line).

Next, we analyzed the illness-recovery processes in the phase plane. In the absence of external disturbances, the gut microbiota stayed in the stable state P_1 (in the R_1 region) to maintain a functional balance in a healthy intestinal system. Once the host infected diseases, the amount of pathogens increased accordingly, resulting in a decrease in the probiotic amount. The orbit crossed the manifold m_1 to the R_2 region (red trajectory ① in Figure 4). In the first 15 illness-treatment processes, 3-day antibiotic intakes could push the trajectory across m_1 and back to the R_1 region (sky blue trajectory ② in Figure 4A). After withdrawing antibiotics, the orbits may automatically return to the healthy stable state P_1 (blue trajectory ④ in Figure 4A), because the orbit started from the R_1 region. However, in the 16^{th} treatment process, 3-day antibiotic treatment could not push the trajectory back to the R_1 region (trajectory ② in Figure 4B). Therefore, the orbit automatically went to the illness stable state P_3 (trajectory ④ in Figure 4B), because it started from the R_2 region. In the

16^{th}, if we used long-term (even permanent) treatment, the trajectory still could not go back to the R_1 region, and finally went to an illness state (trajectory ② in Figure 4C). If FMT combined with antibiotic (Figure 4D) was applied, the state was relocated to the R_1 region (sky blue trajectory ②, and green trajectory ③), and then the orbit automatically returned to the healthy stable state P_1 (trajectory ④). In summary, the system could reach a stable healthy state (P_1) if and only if the microbiota composition state was transferred to the curable region (R_1) by treatments. In this 2-D system, the microbial composition state always returned to the same state after repeated antibiotic perturbations (first 15 times). However, many studies have confirmed that the gut microbiota just returns to a stable state similar to that of the pretreatment state [4, 5, 10].

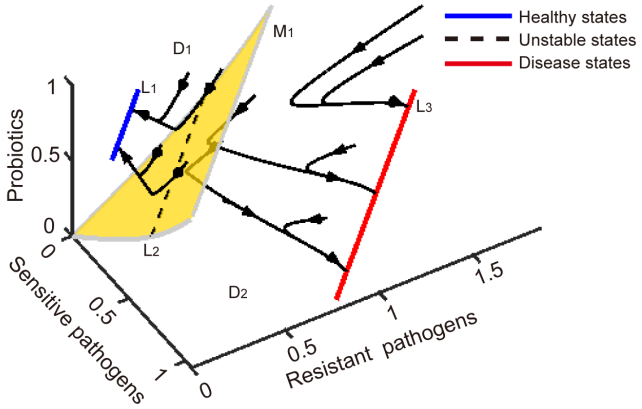

Figure 5. The system dynamics behavior in the 3-D phase space. Eigenvalues of equilibrium states in the line segment L_1 (blue line segment) and L_3 (red line segment) are two negative roots and one zero; but in L_2 (black dashed line segment) are one negative root, one positive root and one zero. The yellow 2-D surface M_1 is formed by the stable manifolds of equilibrium states in L_2, which divides the space into the D_1 domain and D_2 domain.

To test this phenomenon (i.e., the post-antibiotic state is similar to only the pre-treatment state), we further analyzed the dynamic behavior of a 3-D system. Instead of three isolated steady states $P_1 - P_3$ in the 2-D system, there are three types of steady states ($L_1 - L_3$) in the 3-D system (Figure 5). The 3-D phase space in Figure 5A depicts the long-term behavior depending on different initial values. The blue line segment L_1 and red line segment L_3 represent healthy equilibrium states and disease equilibrium states, respectively. The stable manifold (M_1) of the unstable steady states in L_2 is a 2-D surface in the 3-D phase space. The surface M_1 divides the space into two domains (D_1 and D_2). These trajectories from the initial points in D_1 converged towards stable healthy states in L_1, but these trajectories from D_2 ultimately reached a stable disease state in L_3.

Furthermore, we reproduced the first 15 effective treatments (Figure 6A) and the outcomes of different treatments after the 16^{th} illness (Figure 6B-D) in the 3-D phase space. For succinctness, only the first, 10^{th}, 12^{th} and 15^{th} effective treatments are illustrated to show the illness-treatment-recovery process (Figure 6A). During the illness stage, the trajectory went away from the healthy state in L_1, and passed the critical interface M_1 to enter the D_2 domain. Three-day antibiotic intakes could push the trajectory back to the D_1 domain. After the withdrawal of antibiotics, the trajectory eventually

returned to a healthy stable state in L_1, but in a location slightly different from that pretreatment. Furthermore, the recovered healthy states gradually deteriorated (the amount of resistant pathogen increased) with repeating antibiotic treatments (Figure 6A).

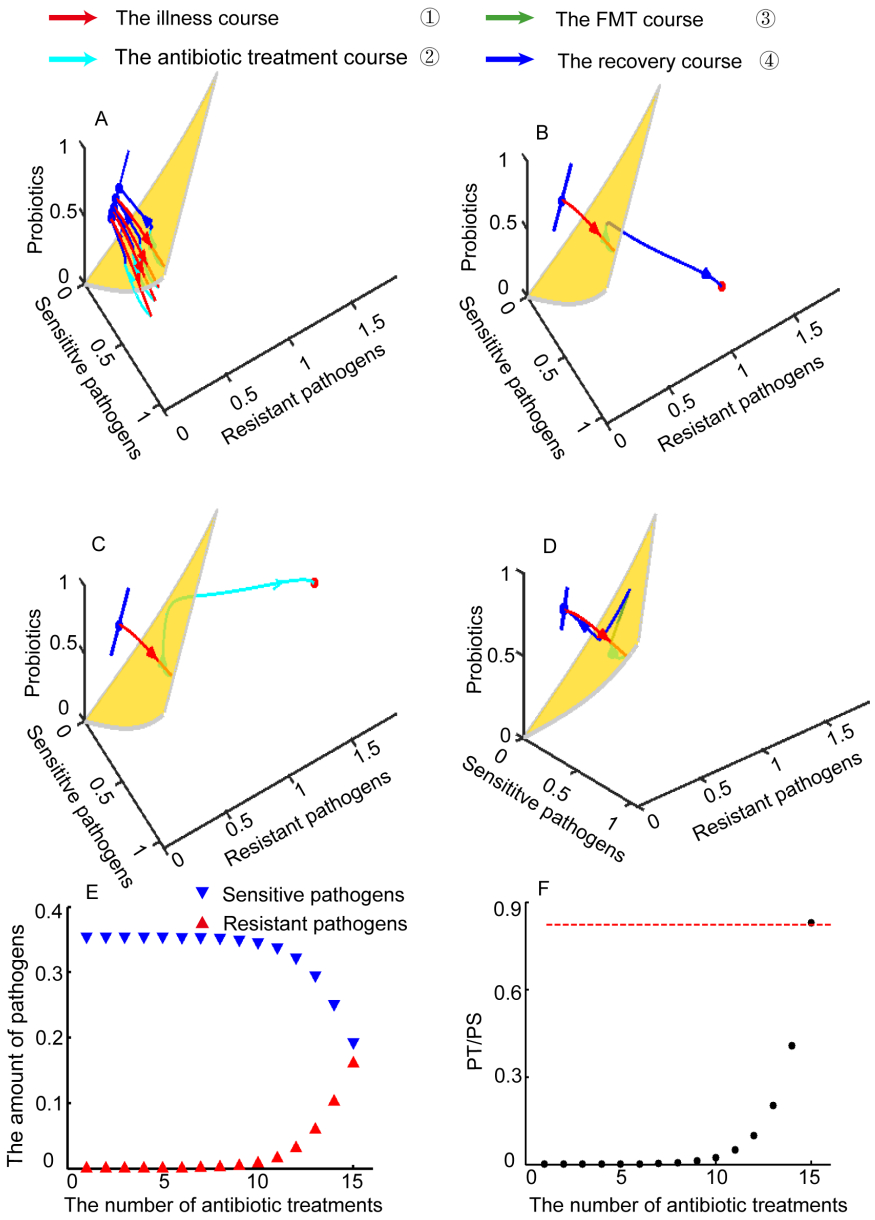

Figure 6. The illness-treatment processes in 3-D phase space. (A) The first 15 infection-treatment processes. (B) The 16^{th} infection was not prevented by a 3-day medication course. (C) The 16^{th} infection was not prevented by a 4-month medication course. (D) The 16^{th} was eliminated by FMT combined with antibiotic. The characteristic of antibiotic resistance is that the trajectory of antibiotic treatment never crosses the yellow surface. (E) The amount of resistant and sensitive pathogens after each drug treatment. (F) The ratio of resistant pathogens to sensitive pathogens in healthy states.

During the 16^{th} illness- treatment- recovery processes, the system eventually reached a disease stable state in L_3, because the trajectory did not cross the critical interface (M_1) after 3-day antibiotic (Figure 6B) or even permanent treatment (Figure 6C). However, after FMT combined with antibiotic treatment, the orbit reached a healthy stable state in L_1 (Figure 6D). In fact, the state was relocated to the D_1 domain by this combined strategy.

As shown in Figure 6A, the recovered healthy states gradually moved along L_1 with repeated antibiotic treatments. From the perspective of pathogen composition, the amount of sensitive bacteria among pathogens gradually decreased, while the amount of resistant pathogens gradually increased with repeated antibiotic perturbations (Figure 6E). Antibiotic resistance emerges when the amount of resistant pathogens reaches a certain level. We used the ratio of resistant pathogens to sensitive pathogens in the healthy stable state to quantify the cumulative effects of repeating antibiotic disturbances. As shown in Figure 6F, this ratio (black dots) gradually increased, and finally passed a critical value (red dashed line) to achieve antibiotic-resistance.

These simulations show that every antibiotic treatment can change the location of the healthy stable state in L_1, e.g., antibiotic treatment can permanently change the steady state ratio of resistant pathogens to sensitive pathogens. These results are consistent with the existing experimental observation that after antibiotic withdrawal, the change in the microbial composition state caused by antibiotics will persist for years or decades [4, 5]. Repeating antibiotic treatments pushed the ratio towards the "bad" direction; that is, resistant pathogens in the post-recovery stable state increased in abundance. When the ratio of resistant pathogens to sensitive pathogens exceeds a threshold value, the antibiotic resistance of the gut microbiota emerges. This model affirmed that the successive shift of post-recovery stable states on L_1 was essentially the change of the ratio (P_T to P_S).

In summary, every antibiotic treatment will permanently change the steady state ratio of sensitive pathogens to resistant pathogens. This small change is the foundation of development of antibiotic resistance. The effects of antibiotic intake will gradually accumulate. Due to the accumulation of the antibiotic effect, the ratio of sensitive pathogens to resistant pathogens continues to changing and eventually exceeds a certain value, inducing the development of antibiotic resistance.

3.3. Key factors affecting antibiotic resistance

In the above analysis, we confirmed that the ratio of sensitive pathogens to resistant pathogens is the root cause of antibiotic resistance. Therefore, we first studied how the initial pathogen composition influences the development of resistance. In Figure 7A, the x-axis stands for the initial ratio of sensitive pathogens to resistant pathogens in healthy individuals. The number of effective antibiotic treatments (before 3 days of antibiotic treatment failed) increased logarithmically with the initial ratio. Every antibiotic treatment increases the ratio of resistant pathogens to sensitive pathogens, until the ratio reaches a threshold to form the resistance. A higher initial ratio indicates a shorter distance to the threshold and fewer effective treatments before resistance than those for a lower initial ratio. Therefore, the initial pathogen composition structure is crucial in determining resistance.

In fact, probiotics also play an important role in the development of antibiotic resistance. Here, we further explored the risk of antibiotic resistance in different microenvironments of the intestinal microbiota. Usually, a higher level of beneficial bacteria means a better microenvironment because beneficial bacteria can inhibit the growth of pathogens. In our model, we used the growth rate of beneficial bacteria, which determines the beneficial bacteria amount in the healthy state, to describe

the microenvironment of different hosts.

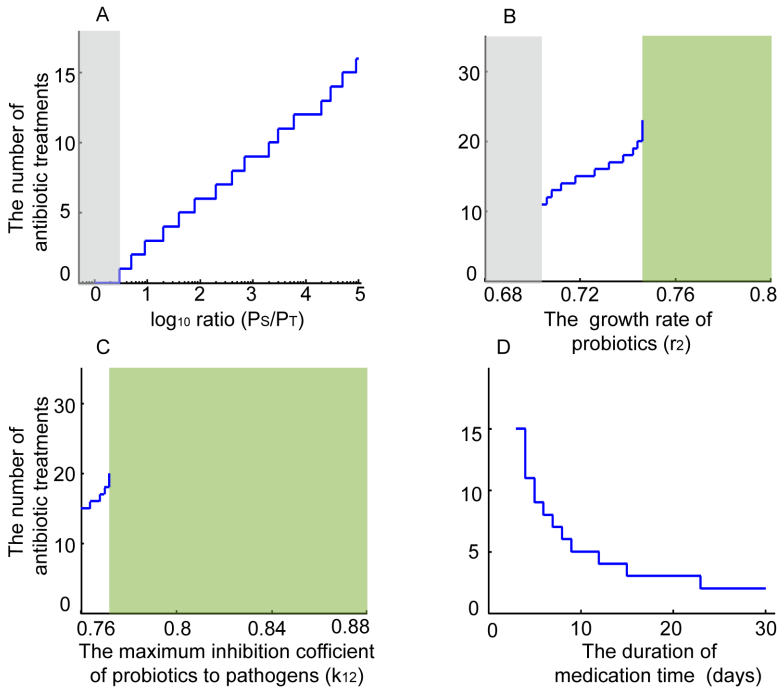

Figure 7. Key factors affecting antibiotic resistance. (A) The pathogen composition in healthy stable states. (B-C) The impact of probiotics on drug resistance. (D) The excessive administration of antibiotics. Here, the gray regions indicate that antibiotic treatment for 3 days failed to eliminate the first infection. The blue line charts indicate that the total number of effective treatments was limited. The green regions show that 3-day antibiotic treatment was permanently effective.

We simulated the total number of effective treatments in different microenvironments. The results show that the number of antibiotic treatments increased with an increasing reproduction rate (r_2) in a small window between the gray region and the green region (Figure 7B). When the reproduction rate of probiotics was relatively small, antibiotic resistance emerged in the first treatment stage (the gray region in Figure 7B). However, when the reproduction rate of probiotics was high, 3-day antibiotic treatment remained effective and resistance never emerged (the green region in Figure 7B).

In addition to the amount of beneficial bacteria, the composition of beneficial bacteria may also be different in different hosts. In our model, we assumed that different compositions of beneficial bacteria can alter the maximum inhibition coefficient of probiotics to pathogens. Then, we explored the number of antibiotic treatments with different inhibition coefficients. Similarly, we also found that increasing the inhibition intensity of probiotics to pathogens could prolong the number of antibiotic treatments to varying degrees (Figure 7C).

Taken together, these simulations show that beneficial bacteria are indispensable in the intestinal flora composition. Enhancing the level or optimizing the endogenous composition of beneficial bacteria can effectively delay or even prevent (depending on the parameters) the development of antibiotic resistance.

Moreover, excessive administration (longer medication duration) of antibiotics had an important effect on the development of antibiotic resistance (Figure 7D). The x-axis represents the duration of antibiotic administration in a course of treatment. In contrast to the initial ratio of pathogens, the number of antibiotic treatments decreased logarithmically with the duration of antibiotic administration. Compared with standard treatment, prolonged antibiotic treatment could accelerate the change in the ratio of sensitive pathogens to resistant pathogens. In other words, excessive administration of antibiotics could promote the development of antibiotic resistance. Therefore, following the medication guidelines or the doctor's advice is very important.

Next, from the perspective of drugs, we explored their effects on antibiotic resistance. Since the application of penicillin in the clinic in 1940, the number of antibiotics has reached several thousand, and there are several hundred commonly used antibiotics in clinical practice. The gut microbiota has different responses to these antibiotics. Therefore, we studied the effect of different antibiotics, which corresponds to different parameter values of η_1, η_2 and η_3 in our model.

Here, we explored the risk of antibiotic resistance from two aspects. The first aspect is that of the bactericidal rates against resistant pathogens. Here, we fixed the bactericidal rate of antibiotics against sensitive pathogens ($\eta_2 = 0.086$) and probiotics ($\eta_3 = 0.015$) and tested the resistance risk of different antibiotics (with different bactericidal rates for resistant pathogens, i.e., η_2).

Generally, extending the antibiotic medication time may cure the illness. In our model, resistance meant that the infection cannot be cured even under endless antibiotic treatment. Therefore, we observed the medication time (may be finite or infinite days) of achieving an effective treatment to determine whether antibiotic resistance emerged.

Under the conditions of Figure 8A ($\eta_2 = 0.016$), the medication time, T, was three days to achieve an effective treatment in the first eighteen infection-treatment processes. In the nineteenth treatment, the required medication time to achieve an effective treatment was prolonged to 4 days. In the twentieth infection, the required medication time was further extended to 9 days (Figure 8A). Furthermore, the antibiotic resistance emerged in the twenty-first treatment stage. We call this type of antibiotic resistance response incurable resistance because treatment failed even with permanent medication.

Under a different parameter value, $\eta_2 = 0.044$ (Figure 8B), the required medication time was gradually extended as the infection time increased. Starting from the forty-first infection, the system could always return to a healthy stable state after a 5-day treatment. Therefore, the gut microbiota did not develop incurable resistance to this antibiotic ($\eta_2 = 0.044$). Here, we call this type of antibiotic resistance responses a curable antibiotic resistance response or pseudorandom resistance.

In our model, we defined the culminating medication time as the required maximum medication time for a specific antibiotic. Hence, the culminating medication time for specific antibiotic ($\eta_2 = 0.016$) was infinity and the culminating medication time was 5 when $\eta_2 = 0.044$.

These simulations (Figure 8A and 8B) implied that the bactericidal rate (η_2) may be a key factor determining the risk of antibiotic resistance. The culminating medication time can be used an effective indicator to measure the resistance of antibiotics. We further studied the culminating medication time for different antibiotics (i.e., different η_2 values) (Figure 8C). Simulation result showed that a critical threshold (black dashed line) of the bactericidal rate (η_2) did exist. When η_2 exceeded the critical threshold, the culminating medication time was finite and was a decreasing function of η_2 (red polygonal line). When η_2 was below the critical threshold, the culminating medication time was infinite (gray region). This meant that the incurable antibiotic resistance is bound to occur.

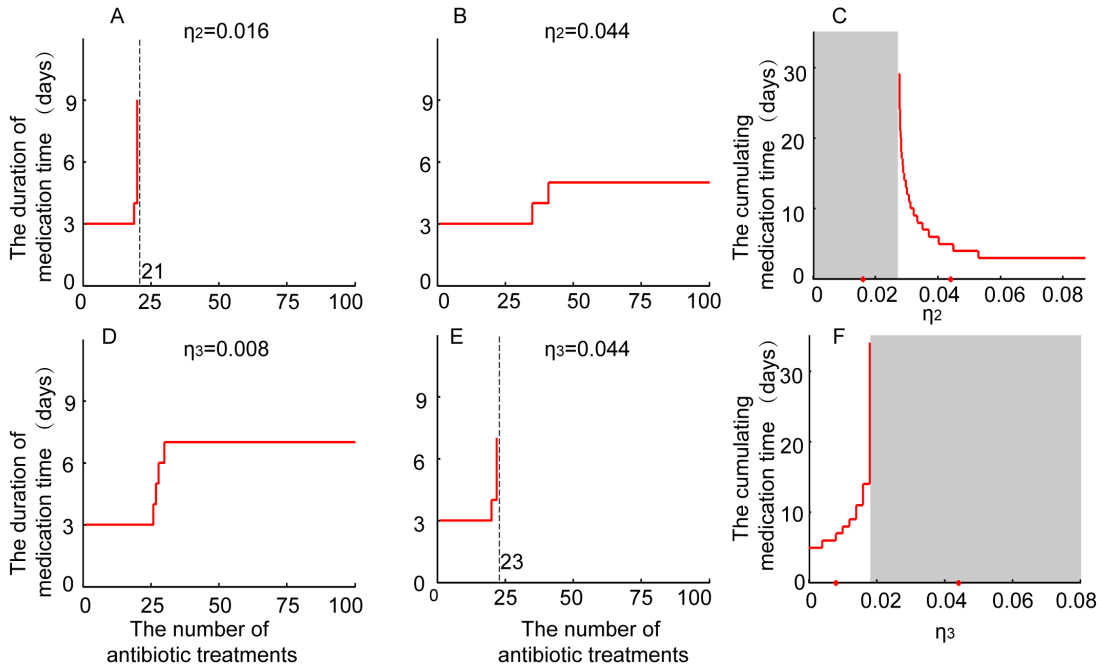

Figure 8. The antibiotic resistance response for different antibiotics. (A-C) η_1 and η_3 are fixed; η_2 is different ($\eta_1 = 0.086, \eta_3 = 0.015$). (D-F) η_1 and η_2 are fixed; η_3 is different ($\eta_1 = 0.086, \eta_2 = 0.03$). (A) and (E) show permanent antibiotic resistance. (B) and (D) show pseudo-resistance. (C) and (F) show the culminating medication time for varying, η_2 and η_3 values, respectively. The purple indicates that the gut microbiota can develop antibiotic resistance for specific antibiotics.

The second aspect is that of bactericidal rates against beneficial bacteria (i.e., different η_3 values). Therefore, we fixed the bactericidal rate of antibiotics against sensitive pathogens ($\eta_1 = 0.086$) and resistant pathogens ($\eta_2 = 0.03$) and explored the effect of different η_3 values on antibiotic resistance. Similarly, our simulations presented two different types of antibiotic resistance responses.

Under the conditions of Figure 8D ($\eta_3 = 0.008$), the medication time was three days to achieve an effective treatment in the first twenty-five infection-treatment processes. Beginning with the twenty-sixth treatment, the required medication time began to increase gradually from 4 days to 7 days. The culminating medication time was 7 days. In contrast, under the conditions of Figure 8E ($\eta_3 = 0.044$), the culminating medication time was infinity.

We also explored the culminating medication time for different bactericidal rates against beneficial bacteria (i.e., η_3). Simulation result showed that the critical threshold (black dashed curve in Figure 8F) of η_3 existed. When η_3 was below the critical threshold, the culminating medication time was finite and was an increasing function of η_3 (red polygonal line). When η_3 exceeded the critical threshold, the culminating medication time was infinite (gray region).

Altogether, a good antibiotic should have a stronger bactericidal rate against resistant pathogens and a weaker bactericidal rate against probiotics. Therefore, our model can also be recommended for optimizing the design of pharmaceutical compositions so that antibiotics have precise lethality.

3.4. *Effective treatment strategies against resistance: FMT combined with antibiotic pretreatment*

In recent decades, clinical practices and mouse models have proven that a burgeoning therapeutic strategy (i.e., FMT) can effectively treat infections caused by resistant pathogens [12–14]. However, the fundamental mechanism of FMT in reshaping the gut microbiota has not been fully elucidated and there also remains a knowledge gap on how to improve FMT efficiency.

To determine the benefits of FMT, we compared the therapeutic efficacy of two different strategies (i.e., permanent antibiotic treatment and FMT combined with antibiotic treatment) in the P-B plane. Here, the horizontal axis P is the total amount of resistant pathogens and sensitive pathogens (i.e., $P = k_1 * P_S + k_2 * P_T$) and the vertical axis B is the amount of the beneficial bacteria. Before the 16^{th} infection, the microflora composition remained in the healthy stable state P_1 (blue dot). After infection, the population of pathogens rapidly reproduced and grew in size, resulting in a decrease in the amount of non-pathogens. The orbit crossed the manifold m_1 to enter the R_2 region (red trajectory ① in Figure 9). In the pure antibiotic treatment, permanent antibiotic therapy was used to eliminate the infection (Figure 9A). The trajectory eventually stabilized to a disease state because this treatment failed to push the trajectory (sky blue trajectory ② in Figure 9A) back into the R_1 region. This result implied that the 16^{th} infection was a resistant infection.

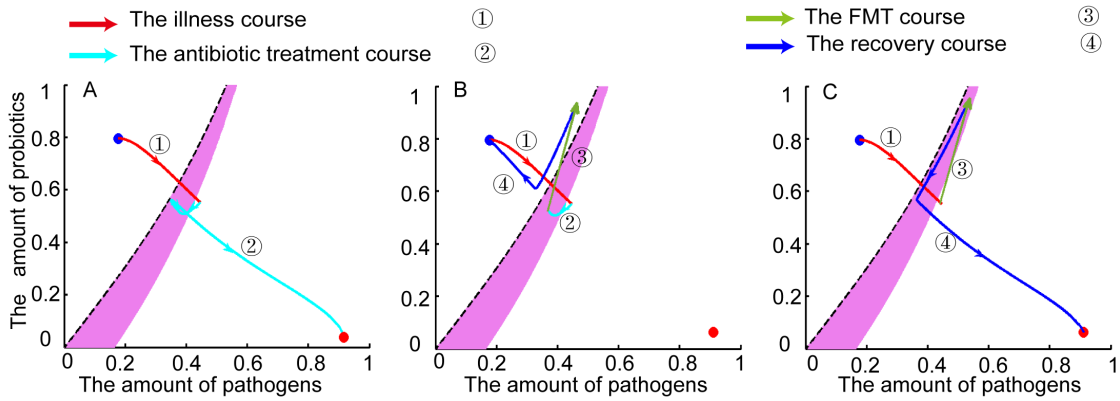

Figure 9. The therapeutic efficacy of three treatment strategies against the 16^{th} infection. (A) Permanent antibiotic treatment. (B) 3-day antibiotic pretreatment combined with FMT. (C) FMT alone. The pink region is the onset range of FMT (k=0.5).

Furthermore, we tested the efficacy of FMT combined with antibiotic therapy in eliminating the 16^{th} infection. We assumed that the donor fecal microbiota has a healthy stable state (denoted as (P_{Sh}, P_{Th}, B_h) corresponding to (P_h, B_h) in the 2-D system). This assumption is because most healthy hosts have a similar "core microbiota". In addition, some studies have pointed out that many factors (such as bowel preparation for the procedure, fresh and frozen material, administration, methods of microbiota preparation and the source of fecal microbiota) may affect the efficiency of FMT [14, 44–48]. To make our model more realistic, we introduced the survival rate k $(0 < k < 1)$ to characterize the transplant survival rate of the donor fecal microbiota. The fecal bacteria injection transfers the transient state (P, B) to a new state (P, B) $+k$ (P_h, B_h). Therefore, the original location of (P, B) is a decisive factor in determining whether the system state $(P, B) + k$ (P_h, B_h) falls into the R_1 region after

FMT, when the colonization rate k is fixed. In addition, we defined the onset range (the purple pink region) of a single FMT which consists of many states in the phase plane. These states (P, B) within the onset range could be transferred to the R_1 region by a single FMT. In Figure 9B, the treatment effect of FMT with antibiotic is shown: first, the trajectory of infection crossed the manifold m_1 to enter the R_2 region (red trajectory ①); second, the 3-day antibiotic pretreatment pushed the trajectory into the onset range (sky blue trajectory ②); third, FMT pulled the trajectory back to the R_1 region (green trajectory ③); and finally, the trajectory (blue trajectory ④) stabilized to the healthy stable state P_1.

Combining the above two therapeutic effects, it can be identified that the large number of probiotics from donors is a key factor affecting the therapeutic effect of FMT. The overwhelming advantage of probiotic to pathogen abundances ensured that the vector k (P_h, B_h) pointed roughly upward in the 2-D phase plane. Therefore, the upward- driven force caused by FMT facilitated the system state crossing the boundary m_1 to enter the R_1 region.

Antibiotic pretreatment in the combined therapy is also very important. Compared to FMT combined with antibiotic therapy, the 16^{th} infection could not be eliminated by using FMT alone. The system transient state (P_d, B_d) after infection fell out of the onset range so that the trajectory of FMT (green trajectory ③ in Figure 9C) did not cross the manifold m_1. Thus, the system finally stabilized to the disease stable state P_3. However, 3-day antibiotic pretreatment could push the trajectory (sky blue trajectory ② in Figure 9B) into the onset range of FMT so that it successfully crossed the manifold m_1 to enter the R_1 region after a single FMT (green trajectory ③ in Figure 9B). Altogether, antibiotic pretreatment is also another key factor in determining the therapeutic efficacy of combined therapy (FMT with antibiotic) by facilitating the transition of the system state into the onset range.

Therefore, the mechanism of action of FMT combined with antibiotic is essentially a synergistic effect of antibiotic pretreatment and FMT. On the one hand, antibiotic pretreatment reduced the amount of whole microbiota (i.e., decreased P and B, respectively), thereby improving the effect of FMT. On the other hand, a large number of probiotics (in the fecal microbiota of donors) ensured that the direction of transplantation (i.e., (P_h, B_h)) pointed roughly upward in the 2-D phase plane. These simulation results are consistent with experimental phenomena; that is, antibiotic pretreatment promotes the successful colonization of the transplanted bacteria in the host [41, 49].

3.5. Advantages of early usage of FMT

In the above analysis, we confirmed that the use of FMT can effectively fight diseases that are resistant to antibiotics. In this section, we will explore the long-term effects of early usage of FMT (with antibiotic) on the formation of antibiotic resistance by examining the total number of treatments.

We first analyzed the total number of treatments for two different strategies, pure antibiotic treatment and FMT combined with antibiotic (Figure 10A) under a specific antibiotic and survival rate. In our previous analysis, FMT was used only after the system had revealed antibiotic resistance (Figure 4D or 6D). Here, FMT was used in advance, for example, after the first infection or second infection, to test the benefits of early application of FMT. In Figure 10A, the x-axis indicates the i-th infection from which the transplantation starts. For example, the 7-th infection indicates that the first 6 illnesses were treated with antibiotic; from the seventh infection, the host was treated with FMT combined with antibiotic. The y-axis is the total number of effective treatments. Additionally, we used the orange and blue bars to distinguish FMT combined with antibiotic treatment and antibiotic treatment, respectively. If FMT combined with antibiotic was used from the first illness, the treatment strategy could be used

up to 35 times (the first bar). If FMT combined with antibiotic was used after using antibiotic 5 times, this strategy could be used only 24 times (the 6-th blue bar). Since the sixteenth infection, the standard antibiotic treatment was no longer effective (gray area). However, usage of FMT combined with antibiotic still could achieve 6 effective treatments (the 16-th orange bar). These simulation results indicate that early usage of FMT can delay the development of antibiotic resistance.

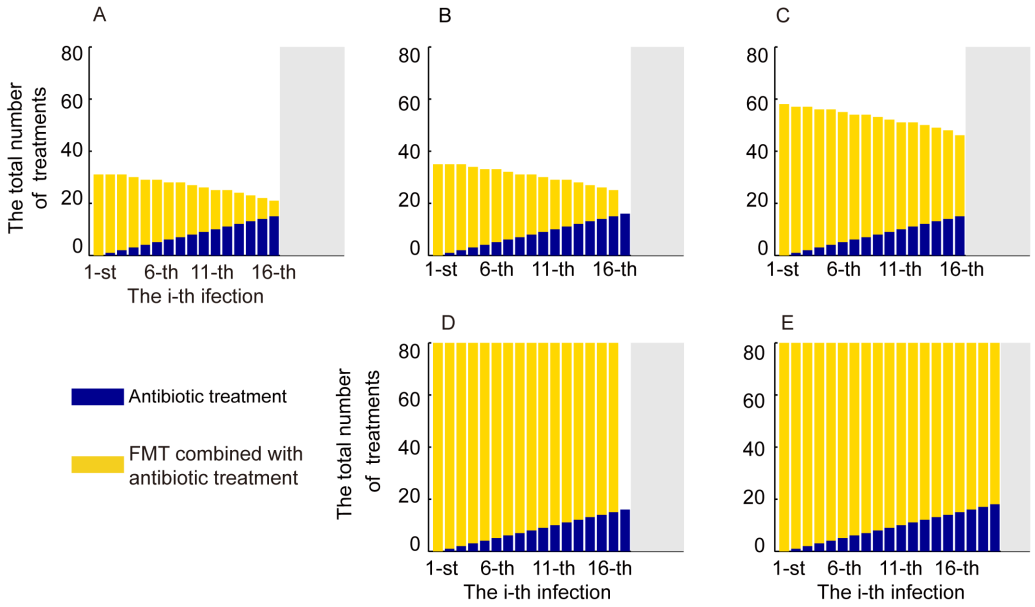

Figure 10. The advantage of early usage of FMT. The blue bars represent the number of pure antibiotic treatments (i.e., antibiotic treatment without FMT). The orange bars represent the number of FMT combined with 3-day antibiotic treatments (i.e., FMT combined with antibiotic). The gray region indicates that the two treatments are ineffective. The x-label (i) indicates that the first i-1 illnesses are treated with antibiotic; beginning from the i-th infection, the host is then treated with FMT combined with antibiotic. (A) $k = 0.5, \eta_2 = 0.0016$. (B) $k = 0.5, \eta_2 = 0.003$. (C) $k = 0.5263494, \eta_2 = 0.0016$. (D) $k = 0.51, \eta_2 = 0.003$. (E) $k = 0.43, \eta_2 = 0.012$.

The above results are based on parameters in Table 1. These parameters, especially the bactericidal rate of antibiotics and the survival rate (i.e., η_j and k) may vary in the real environment. Therefore, the effect of early usage of FMT combined with antibiotic requires further study in a broad parameter space. Simulation results (different η_2 and k values) show different typical cases. Under some parameters, the systems eventually exhibited resistance to FMT combined with antibiotic (Case A). However, under other parameters, the systems never exhibited resistance to FMT (with antibiotic) (Case B). In some situations, use of FMT combined with antibiotic could rescue the treatment after antibiotic resistance emergence (Case II), but in other situations even FMT combined with antibiotic failed (Case I). In all these typical cases (Case A-I in Figure 10B, Case A-II in Figure 10C, Case B-I in Figure 10D and Case B-II in Figure 10E), early usage of FMT could extend the number of effective treatments, compared with those of FMT combined with antibiotic use after resistance emergence.

For Case A-I, after 16 treatments with antibiotic, antibiotic resistance emerged (gray region in Figure 10B) under certain parameters. If FMT combined with antibiotic was used first after resistance emergence, the treatment could not be rescued (the 17-th bar). However, if FMT combined with antibiotic was used beginning at the sixteenth infection, it could be used 10 times (the 16-th orange bar). If the combined treatment was used beginning at the first infection, the total number of effective treatments was 35 (the 1-st bar). The total number of effective treatments will be prolonged only if FMT is used in advance.

For Case A-II, after 15 treatments with antibiotic, antibiotic resistance emerged (gray region in Figure 10C) under certain parameters. Unlike Case A-I, if FMT combined with antibiotic pretreatment was first used after resistance emergence, the treatment could be rescued, and up to 30 effective treatments were achieved (the 16-th orange bar). If FMT combined with antibiotic was first used beginning at the eleventh infection, it could be used 41 times (the 11-th orange bar). If the combined treatment was used from the first infection, the total number of effective treatments was 58 (the 1-st bar). Regardless of whether early FMT (with antibiotic) was employed, it always extended the number of effective treatments.

For Case B-I, antibiotic resistance emerged (gray region in Figure 10D) after 16 treatments with antibiotic. If FMT combined with antibiotic pretreatment was first used after resistance emerged, the treatment could not be rescued (the 17-th bar). However, if the combined treatment was used in advance, the treatment was permanently effective (for example, the 16-th orange bar).

For Case B-II, after 18 antibiotic treatments, antibiotic resistance emerged (gray region in Figure 10E). If FMT combined with antibiotic pretreatment was first used after resistance emergence, the treatment could be rescued. Moreover, the treatment was permanently effective (the 19-th orange bar).

All of the above four typical cases indicated that the early use of FMT combined with antibiotic pretreatment can significantly delay antibiotic resistance emergence (Figure 10A-E). Furthermore, in some cases, early use of the combined therapy could even permanently prevent the development of antibiotic resistance (Figure 10D-E). These results suggest that early usage of FMT combined with antibiotic could be recommended for clinical treatment.

3.6. Exploring the onset range of multiple FMTs

In our model, we used FMT combined with 3-day antibiotic pretreatment to simulate the clinical recovery treatment protocol, antibiotic pretreatment combined with a single FMT. In clinical trials, feces dilutions by the donor were infused into the patient through a nasoduodenal tube (2 to 3 minutes per 50 ml) and the tube was removed after 30 minutes [15]. A single FMT in clinical treatment was usually used to treat patients with *Clostridium difficile* infection or refractory intestinal infection. However, some diseases require multiple FMTs, such as Crohn's disease or ulcerative colitis [50–52].

Next, we clarified whether multiple FMTs are superior to a single FMT. In fact, the onset range of multiple FMTs directly reflects the corresponding curable range. Therefore, we analyzed the variety of onset ranges in the phase plane (P - B). Here, the onset range consisted of those states that can be transferred to the R_1 region by multiple FMTs. A single FMT pushed the transient state (P, B) in the R_2 region up to a new state $(P, B) + k\ (P_h, B_h)$ along the vector (P_h, B_h) (green arrow in Figure 11A). Therefore, the critical curve of a single FMT (red curve) is obtained directly by moving the manifold m_1 downward by $k\ (P_h, B_h)$. The upper left region (red) surrounded by the boundary and manifold

(m_1) is the onset range of a single FMT. Here, we assumed that the second FMT was performed on the second day after the first FMT. The corresponding boundary (two FMTs) was not simply obtained by moving the boundary (the first FMT). Therefore, we simulated the process to obtain the onset range of two FMTs (green). Generally, the onset range of two FMTs was bigger than that of a single FMT. Similarly, the onset range of n-FMT was larger than that of n-1 FMTs. This implies that multiple FMTs are better than a single FMT (Figure 11).

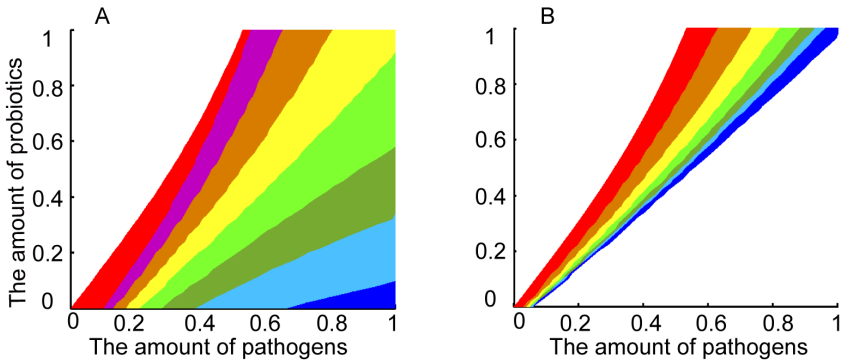

Figure 11. The effective region of multiple FMTs for different survival rates. (A) The effective region of finite FMTs covers the whole region of R_2. $k = 0.3$; here, different colors represent the magnitude of increase of the onset range (every FMT). (B) The effective region of infinite FMTs covers the partial region of R_2. $k = 0.07$; here, different colors represent the magnitude of the increase of the onset range (every 5 FMTs).

Since the onset range for every FMT is increasing, whether the corresponding onset range of infinite FMTs can cover the whole non-self-healing area (R_2) remains to be further explored. In fact, there may be different cases. As shown in Figure 11A, the onset range of finite FMTs can fully cover the whole region of R_2. However, under other parameters, the onset range of infinite FMTs can cover only a local region of R_2 (Figure 11B). Further observation showed that the increase in the onset range (each FMT) gradually decreased in the second case, while in the first case, the opposite was true.

Altogether, these results show that multiple FMTs have a wider therapeutic range than a single FMT. Therefore, multiple FMTs can be recommended for the treatment of some serious infections or infections caused by "superbugs".

3.7. The impact of a donor's medication history on FMT

In the above analysis, fecal microbiota from donors with no history of medication was used for the microbiota of transplantation. However, in the real life, donors with no history of medication are quite rare. The fecal material may come from different donors, i.e., the composition of pathogens or probiotics is different. The transplant microbiota may also come from the same donor, i.e., the composition of pathogens and probiotics are the same but the composition of resistant pathogens and sensitive pathogens is different. In this section, we will explore the second case, in which a different composition of pathogens is caused by repeating antibiotic treatment.

Next, we analyzed the corresponding total number of treatments with FMT combined with antibiotic pretreatment (in the second case) in Figure 12A. Here, the x-axis and z-axis represent the i-th infection and the total number of FMT combined with antibiotic treatments, respectively. For instance, the 6-th bars indicate that patients were treated with the combined therapy from the sixth infection. From the x-z plane, it can be seen that the sooner FMT is used, the greater the number of FMT treatments is. The y-axis represents the number of times the donors have taken medicine. For example, 5-D denotes fecal material from donors that have taken medicine five times. From the y-z plane, we can see that the fewer number of times the donors take medicine (in Figure 12A y-axis), the greater the number of FMT treatments is.

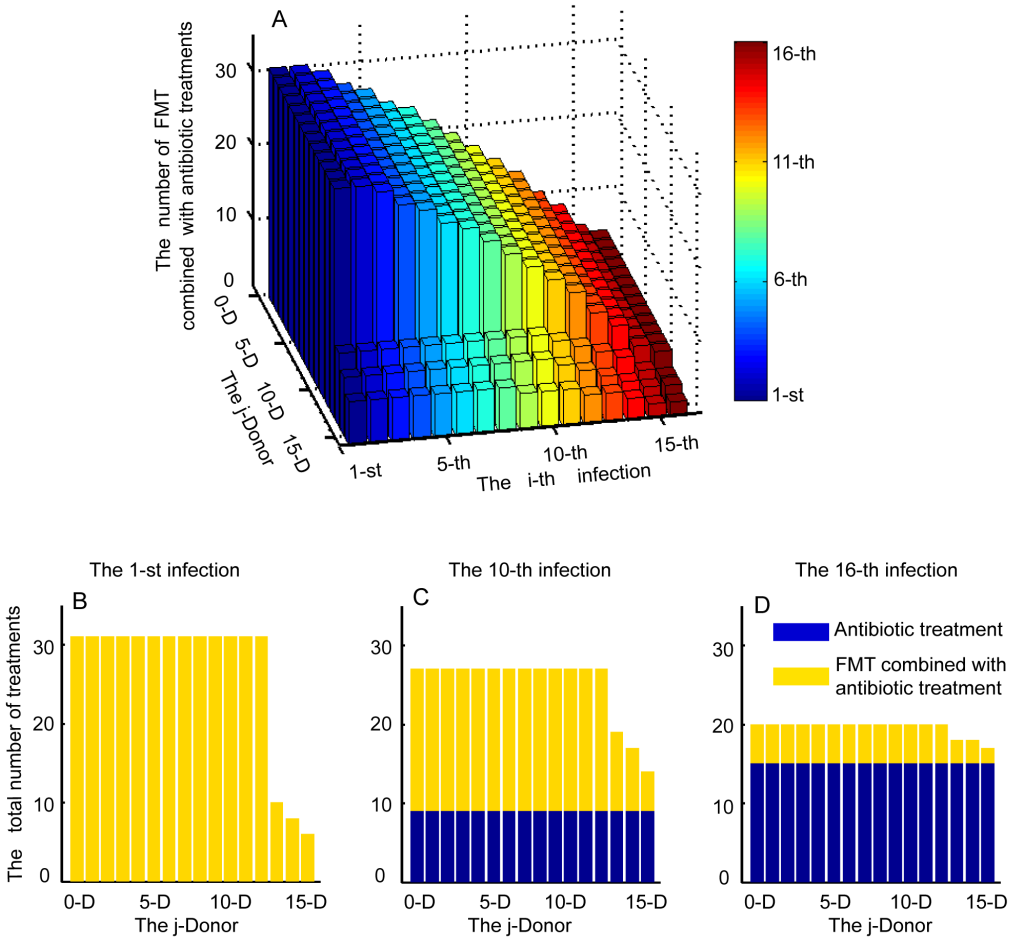

Figure 12. The impact of different donors' fecal microbiota on FMT. (A) Early use of FMT combined with antibiotic and fecal microbiota from donors that have taken medicine several times. The color bar represents the results of fecal bacteria transplantation from the i-th infection. (B) FMT combined with antibiotic is used beginning at the first infection. (C) FMT combined with antibiotic is used beginning at the tenth infection. (D) FMT combined with antibiotic is used beginning at the sixteenth infection.

Furthermore, we explored the corresponding total number of treatments for early use of FMT combined with antibiotic in comparison with the standard antibiotic treatment. Here, the blue bar indicates the 3-day antibiotic treatment; the orange bar indicates FMT (with antibiotic) treatment. Figure 12B presents the use of FMT (with antibiotic) beginning at the first infection. Surprisingly, when fecal microbiota donors have taken medications less than 13 times, the total number of treatments was the same, despite the use of different fecal microbiota. However, when fecal microbiota donors have taken medicine 13 times or more, the total number of treatments decreased dramatically. We observed similar phenomena even when FMT (with antibiotic) treatments were not used until the 10^{th} (Figure 12C) or even 16^{th} infection (Figure 12D). These simulation results show that early use of FMT (with antibiotic) may accelerate the emergence of antibiotic resistance when fecal microbiota donors have taken medicine several times. This finding may be the reason why screening of donors should first exclude donors with a history of serious illness.

In brief, we confirmed that fecal material should come from donors who have taken fewer medicines. Clinically, the screening criteria should be strictly followed and further combined with "the exclusive method" to obtain the healthiest donors.

4. Conclusions

We established a dynamic microbiota model to describe the comprehensive effects of antibiotic therapy, interspecies inhibition and resource competition on the balance of the intestinal flora. The development of antibiotic resistance was revealed by simulating multiple complete illness - treatment - recovery processes. That is, repeated antibiotic intake promoted the proportion of resistant pathogens and sensitive pathogens in the healthy state to exceed a specific threshold, which led to the emergence of drug resistance.

We believe that the proposed resistance mechanism is also widely applicable in the treatment of other diseases. Drug resistance is commonly seen in various clinical treatments. For example, the first-line treatment of metastatic prostate cancer uses androgen deprivation therapy (ADT), but nearly all men progress to a resistant stage. In metastatic prostate cancer, there are three competing phenotypes: (i) T+ cells are sensitive to ADT; (ii) TP (testosterone producing) cells are sensitive to ADT but also helps T+ cells; and (iii) T− cells are resistant to ADT [53, 54]. This kind of competing structure is similar to our sensitive pathogens / probitcs / resistant pathogens framework. Thus, the mechanism of drug resistance here may be similar to that proposed by us.

Furthermore, our model confirmed that antibiotic resistant infections could be cured based on FMT combined with antibiotic. In particular, the numerical simulation predictions also showed that early usage of FMT can delay or prevent the development of antibiotic resistance. This finding implied that multiple FMTs or early use of FMT may be implemented instead of antibiotic therapy alone to prevent the emergence of antibiotic resistance in the future. Therefore, we should strive to improve fecal microbiota transplantation so that it can be widely used in the clinic. Specifically, the screening criteria for fecal bacteria and transplantation techniques need to be improved. Similarly, in the treatment of cancer, some scholars have found that adaptive therapy can delay the emergence of drug resistance more effectively than those of the standard cure or continuous MTD treatment [53]. Therefore, adaptive therapy may also be an effective treatment to delay the development of antibiotic resistance. Besides, some investigations have shown that the prevalence of resistant microbiota

decreased markedly following a reduction in specific antibiotic use in agricultural areas. Hence, we need to standardize and strictly limit the use of antibiotics to reduce the overall outbreak of antibiotic resistance.

The main purpose of this study is to qualitatively explain how drug-resistance emerges upon the accumulation of the effect of antibiotics. Although our mathematical model is rather simple, we maintain the most critical reactions among different intestinal flora in the mathematical model, which is the most essential reason for the mechanism of the emergence of drug-resistance. The mathematical model is still somewhat limited because it is difficult to determine all the real parameter values from experimental data or other literature. Therefore, we evaluate the relative value of some parameters based on the clinical data. For example, the killing rate of antibiotic for sensitive bacteria is larger than other bacteria [55]. Other parameters are determined according to the time scale of the clinical observations and some biological phenomena [56–58]. Regarding to the other limitation of this study, the main approach to reveal the mechanism of drug-resistance is numerical simulations with fixed parameter values. In fact, we also intended to perform some analytical studies upon system (2.2) and system (3.1). However, due to the complexity of the functions in the systems, we can't determine theoretically if all these sufficient conditions can be satisfied at the same time. Therefore, to analysis the stability, we will use piecewise linear system to approximate system (2.2) and system (3.1) in the future work.

Acknowledgments

This work is supported by the National Natural Science Foundation of China (Grant No. 11671417 and 11701405), the Jiangsu Province Science Foundation for Youths (Grant No. BK20170328), and the Priority Academic Program of Jiangsu Higher Education Institutions (Grant No. 5832004317).

Conflict of interest

All authors declare no conflicts of interest in this paper in this section.

References

1. S. Nancey, J. Bienvenu, B. Coffin, et al., Butyrate strongly inhibits in vitro stimulated release of cytokines in blood, *Dig. Dis. Sci.*, **47** (2002), 921–928.
2. S. M. Finegold, S. E. Dowd, V. Gontcharova, et al., Pyrosequencing study of fecal microflora of autistic and control children, *Anaerobe*, **16** (2010), 444–453.
3. A. C. Ericsson, S. Akter, M. M. Hanson, et al., Differential susceptibility to colorectal cancer due to naturally occurring gut microbiota, *Oncotarget*, **6** (2015), 33689–33704.
4. H. E. Jakobsson, C. Jernberg, A. F. Andersson, et al., Short-term antibiotic treatment has differing long-term impacts on the human throat and gut microbiome, *PLoS One*, **5** (2010), e9836.
5. L. Dethlefsen and D. A. Relman, Incomplete recovery and individualized responses of the human distal gut microbiota to repeated antibiotic perturbation, *Proc. Natl. Acad. Sci. U. S. A.*, **108** (2011), 4554–4561.

6. J. J. Faith, J. L. Guruge, M. Charbonneau, et al., The long-term stability of the human gut microbiota, *Science*, **341** (2013), 1237439.
7. I. Gustafsson, M. Sjolund, E. Torell, et al., Bacteria with increased mutation frequency and antibiotic resistance are enriched in the commensal flora of patients with high antibiotic usage, *J. Antimicrob. Chemother.*, **52** (2003), 645–650.
8. D. Artis, Epithelial-cell recognition of commensal bacteria and maintenance of immune homeostasis in the gut, *Nat. Rev. Immunol.*, **8** (2008), 411–420.
9. V. Bucci, C. D. Nadell and J. B. Xavier, The evolution of bacteriocin production in bacterial biofilms, *Am. Nat.*, **178** (2008), E162–173.
10. J. Zheng, M. G. Ganzle, X. B. Lin, et al., Diversity and dynamics of bacteriocins from human microbiome, *Environ Microbiol*, **17** (2015), 2133–2143.
11. F. Zhang, B. Cui, X. He, et al., Microbiota transplantation: concept, methodology and strategy for its modernization, *Protein. Cell.*, **9** (2018), 462–473.
12. S. N. Gopalsamy, M. H. Woodworth, T. Wang, et al., The Use of Microbiome Restoration Therapeutics to Eliminate Intestinal Colonization With Multidrug-Resistant Organisms, *Am. J. Med. Sci.*, **356** (2018), 433–440.
13. Y. Wei, J. Gong, W. Zhu, et al., Fecal microbiota transplantation restores dysbiosis in patients with methicillin resistant Staphylococcus aureus enterocolitis, *BMC Infect. Dis.*, **15** (2015), 265.
14. D. Ishikawa, T. Sasaki, T. Osada, et al., Changes in Intestinal Microbiota Following Combination Therapy with Fecal Microbial Transplantation and Antibiotics for Ulcerative Colitis, *Inflamm. Bowel. Dis.*, **23** (2017), 116–125.
15. E. van Nood, A. Vrieze, M. Nieuwdorp, et al., Duodenal infusion of donor feces for recurrent Clostridium difficile, *N. Engl. J. Med.*, **368** (2013), 407–415.
16. C. Ubeda, V. Bucci, S. Caballero, et al., Intestinal microbiota containing Barnesiella species cures vancomycin-resistant Enterococcus faecium colonization, *Infect. Immun.*, **81** (2013), 965–973.
17. L. J. Brandt, American Journal of Gastroenterology Lecture: Intestinal microbiota and the role of fecal microbiota transplant (FMT) in treatment of C. difficile infection, *Am. J. Gastroenterol.*, **108** (2013), 177–185.
18. M. C. Zanella Terrier, M. L. Simonet, P. Bichard, et al., Recurrent Clostridium difficile infections: the importance of the intestinal microbiota, *World J. Gastroenterol.*, **20** (2014), 7416–7423.
19. S. Jamot, V. Raghunathan, K. Patel, et al., Factors Associated with the Use of Fecal Microbiota Transplant in Patients with Recurrent Clostridium difficile Infections, *Infect. Control. Hosp. Epidemiol.*, **39** (2018), 302–306.
20. G. Cammarota, G. Ianiro and A. Gasbarrini, Fecal microbiota transplantation for the treatment of Clostridium difficile infection: a systematic review, *J. Clin. Gastroenterol.*, **48** (2014), 693–702.
21. Y. Li, A. Karlin, J. D. Loike, et al., Determination of the critical concentration of neutrophils required to block bacterial growth in tissues, *J. Exp. Med.*, **200** (2004), 613–622.
22. A. Heinken and I. Thiele, Anoxic Conditions Promote Species-Specific Mutualism between Gut Microbes In Silico, *Appl. Environ. Microbiol.*, **81** (2015), 4049–4061.

23. T. J. Wiles, M. Jemielita, R. P. Baker, et al., Host Gut Motility Promotes Competitive Exclusion within a Model Intestinal Microbiota, *PLoS Biol.*, **14** (2016), e1002517.
24. T. E. Gibson, A. Bashan, H. T. Cao, et al., On the Origins and Control of Community Types in the Human Microbiome, *PLoS Comput. Biol.*, **12** (2016), e1004688.
25. D. Gonze, L. Lahti, J. Raes, et al., Multi-stability and the origin of microbial community types, *ISME J.*, **11** (2017), 2159–2166.
26. A. L. Gomes, J. E. Galagan and D. Segre, Resource competition may lead to effective treatment of antibiotic resistant infections, *PLoS One*, **8** (2013), e80775.
27. E. M. D'Agata, M. Dupont-Rouzeyrol, P. Magal, et al., The impact of different antibiotic regimens on the emergence of antimicrobial-resistant bacteria, *PLoS One*, **3** (2008), e4036.
28. V. Bucci, S. Bradde, G. Biroli, et al., Social interaction, noise and antibiotic-mediated switches in the intestinal microbiota, *PLoS Comput. Biol.*, **8** (2012), e1002497.
29. S. Estrela and S. P. Brown, Community interactions and spatial structure shape selection on antibiotic resistant lineages, *PLoS Comput. Biol.*, **14** (2018), e1006179.
30. S. W. Wu, H. de Lencastre and A. Tomasz, Recruitment of the mecA gene homologue of Staphylococcus sciuri into a resistance determinant and expression of the resistant phenotype in Staphylococcus aureus, *J. Bacteriol.*, **183** (2001), 2417–2424.
31. S. Gottig, S. Riedel-Christ, A. Saleh, et al., Impact of blaNDM-1 on fitness and pathogenicity of Escherichia coli and Klebsiella pneumoniae, *Int. J. Antimicrob. Agents.*, **47** (2016), 430–435.
32. R. Freter, H. Brickner, J. Fekete, et al., Survival and implantation of Escherichia coli in the intestinal tract, *Infect. Immun.*, **39** (1983), 686–703.
33. M. P. Leatham, S. Banerjee, S. M. Autieri, et al., Precolonized human commensal Escherichia coli strains serve as a barrier to E. coli O157:H7 growth in the streptomycin-treated mouse intestine, *Infect. Immun.*, **77** (2009), 2876–2886.
34. K. Tabita, S. Sakaguchi, S. Kozaki, et al., Comparative studies on Clostridium botulinum type A strains associated with infant botulism in Japan and in California, USA, *Jpn. J. Med. Sci. Biol.*, **43** (1990), 219–231.
35. Y. Yamashiro, Gut Microbiota in Health and Disease, *Ann. Nutr. Metab.*, **71** (2017), 242–246.
36. C. Cordonnier, G. Le Bihan, J. G. Emond-Rheault, et al., Vitamin B12 Uptake by the Gut Commensal Bacteria Bacteroides thetaiotaomicron Limits the Production of Shiga Toxin by Enterohemorrhagic Escherichia coli, *Toxins (Basel)*, **8** (2016), E14.
37. R. A. Sorg, L. Lin, G. S. van Doorn, et al., Collective Resistance in Microbial Communities by Intracellular Antibiotic Deactivation, *PLoS Biol.*, **14** (2016), e2000631.
38. T. Ito, K. Okuma, X. X. Ma, et al., Insights on antibiotic resistance of Staphylococcus aureus from its whole genome: genomic island SCC, *Drug. Resist. Updat.*, **6** (2003), 41–52.
39. H. Nicoloff and D. I. Andersson, Indirect resistance to several classes of antibiotics in cocultures with resistant bacteria expressing antibiotic-modifying or -degrading enzymes, *J. Antimicrob. Chemother.*, **71** (2016), 100–110.

40. C. A. Lozupone, J. I. Stombaugh, J. I. Gordon, et al., Diversity, stability and resilience of the human gut microbiota, *Nature*, **489**, (2012), 220–230.
41. C. Manichanh, J. Reeder, P. Gibert, et al., Reshaping the gut microbiome with bacterial transplantation and antibiotic intake, *Genome. Res.*, **20** (2010), 1411–1419.
42. E. K. Costello, C. L. Lauber, M. Hamady, et al., Bacterial community variation in human body habitats across space and time, *Science*, **326** (2009), 1694–1697.
43. P. J. Turnbaugh, M. Hamady, T. Yatsunenko, et al., A core gut microbiome in obese and lean twins, *Nature*, **457** (2009), 480–484.
44. A. Uygun, K. Ozturk, H. Demirci, et al., Fecal microbiota transplantation is a rescue treatment modality for refractory ulcerative colitis, *Medicine (Baltimore)*, **96** (2017), e6479.
45. B. Cui, Q. Feng, H. Wang, et al., Fecal microbiota transplantation through mid-gut for refractory Crohn's disease: safety, feasibility, and efficacy trial results, *J. Gastroenterol. Hepatol.*, **30** (2015), 51–58.
46. C. R. Kelly, S. Kahn, P. Kashyap, et al., Update on Fecal Microbiota Transplantation 2015: Indications, Methodologies, Mechanisms, and Outlook, *Gastroenterology*, **149** (2015), 223–237.
47. S. Vermeire, M. Joossens, K. Verbeke, et al., Donor Species Richness Determines Faecal Microbiota Transplantation Success in Inflammatory Bowel Disease, *J. Crohns. Colitis.*, **10** (2016), 387–394.
48. H. Seedorf, N. W. Griffin, V. K. Ridaura, et al., Bacteria from diverse habitats colonize and compete in the mouse gut, *Cell*, **159** (2014), 253–266.
49. S. K. Ji, H. Yan, T. Jiang, et al., Preparing the Gut with Antibiotics Enhances Gut Microbiota Reprogramming Efficiency by Promoting Xenomicrobiota Colonization, *Front. Microbiol.*, **8** (2017), 1208.
50. D. L. Suskind, M. J. Brittnacher, G. Wahbeh, et al., Fecal microbial transplant effect on clinical outcomes and fecal microbiome in active Crohn's disease, *Inflamm. Bowel. Dis.*, **21** (2015), 556–563.
51. A. K. Seth, P. Rawal, R. Bagga, et al., Successful colonoscopic fecal microbiota transplantation for active ulcerative colitis: First report from India, *Indian. J. Gastroenterol.*, **35** (2016), 393–395.
52. S. X. Liu, Y. H. Li, W. K. Dai, et al., Fecal microbiota transplantation induces remission of infantile allergic colitis through gut microbiota re-establishment, *World J. Gastroenterol.*, **23** (2017), 8570–8581.
53. J. Zhang, J. J. Cunningham, J. S. Brown, et al., Integrating evolutionary dynamics into treatment of metastatic castrate-resistant prostate cancer, *Nat. Commun.*, **8** (2017), 1816.
54. R. B. Montgomery, E. A. Mostaghel, R. Vessella, et al., Maintenance of intratumoral androgens in metastatic prostate cancer: a mechanism for castration-resistant tumor growth, *Cancer Res.*, **68** (2008), 4447–4454.
55. J. M. Hyatt, D. E. Nix, C. W. Stratton, et al., In vitro pharmacodynamics of piperacillin, piperacillin-tazobactam, and ciprofloxacin alone and in combination against Staphylococcus aureus, Klebsiella pneumoniae, Enterobacter cloacae, and Pseudomonas aeruginosa, *Antimicrob. Agents Chemother.*, **39** (1995), 1711–1716.

56. D. M. Chaput de Saintonge, D. F. Levine, I. T. Savage, et al., Trial of three-day and ten-day courses of amoxycillin in otitis media, *Br. Med. J. (Clin. Res. Ed.)*, **284** (1982), 1078–1081.

57. C. Llor and L. Bjerrum, Antimicrobial resistance: risk associated with antibiotic overuse and initiatives to reduce the problem, *Ther. Adv. Drug Saf.*, **5**, (2014), 229–241.

58. I. van Langeveld, R. C. Gagnon, P. F. Conrad, et al., Multiple-Drug Resistance in Burn Patients: A Retrospective Study on the Impact of Antibiotic Resistance on Survival and Length of Stay, *J. Burn. Care. Res.*, **38**, (2017), 99–105.

AIMS Press